# Catalytic hydrotreatment of pyrolytic lignins from different sources to biobased chemicals

Figueirêdo, M. B.; Deuss, P. J.; Venderbosch, R. H.; Heeres, H. J.

*Published in:*
Biomass and Bioenergy

*DOI:*
10.1016/j.biombioe.2020.105484



*Publication date:*
2020

Biomass and Bioenergy 134 (2020) 105484

Contents lists available at ScienceDirect

Biomass and Bioenergy

journal homepage: http://www.elsevier.com/locate/biombioe

# Catalytic hydrotreatment of pyrolytic lignins from different sources to biobased chemicals: Identification of feed-product relations

M.B. Figueirêdo [a], P.J. Deuss [a], R.H. Venderbosch [b], H.J. Heeres [a,*]

[a] Department of Chemical Engineering, ENTEG, University of Groningen, Nijenborgh 4, 9747, AG, Groningen, the Netherlands
[b] Biomass Technology Group BV, Josink Esweg 34, 7545, PN Enschede, the Netherlands

ARTICLE INFO

*Keywords:*
Pyrolytic lignin
Hydrotreatment
Catalysis
Aromatics
Alkylphenolics

ABSTRACT

The pyrolysis liquid biorefinery concept involves separation of pyrolysis liquids in various fractions followed by conversion of the fractions to value-added products. Pyrolytic lignins (PLs), the water-insoluble fractions of pyrolysis liquids, are heterogeneous, cross linked oligomers composed of substituted phenolics whose structure and physicochemical properties vary significantly depending on the biomass source. The catalytic hydrotreatment of six PLs from different biomass sources (pine, prunings, verge grass, miscanthus and sunflower seed peel) was investigated to determine the effect of different feedstocks on the final product composition and particularly the amount of alkylphenolics and aromatics, the latter being important building blocks for the chemical industry. Hydrotreatment was performed with Pd/C, 100 bar of hydrogen pressure and temperatures in the range of 350–435 °C, resulting in depolymerized product mixtures with monomer yields up to 39.1 wt% (based on PL intake). The molecular composition of the hydrotreated oils was shown to be a strong function of the PL feed and reaction conditions. Statistical analyses provided the identification of specific structural drivers on the formation of aromatics and phenolics, and a simple model able to accurately predict the yields of such monomers after catalytic hydrotreatment was obtained ($R^2$ = 0.9944) and cross-validated ($R^2$ = 0.9326). These feed-product relations will support future selections of PL feeds to obtain the highest amounts of valuable biobased chemicals.

## 1. Introduction

Pyrolysis liquids have great potential for the production of biofuels and biobased chemicals [1]. Nonetheless, raw pyrolysis liquids are acidic, chemically heterogeneous, oligomeric and prone to repolymerization upon storage. As such, efficient upgrading strategies must be developed to, amongst others, depolymerize and deoxygenate the mixtures [2]. Pyrolysis liquids can be either upgraded as a whole or separated first into a sugar and lignin fraction through a simple water fractionation [3]. The latter results in the formation of a lignin-derived insoluble fraction, known as pyrolytic lignin (PL) and a pyrolytic sugar fraction. This initial fractionation is an essential element in a pyrolysis liquid biorefinery [4] (Fig. 1). In this concept, pyrolysis liquids are initially separated into fractions and each fraction is valorized in an integrated process for the production of heat, power, biofuels and bio-based chemicals. Fractionation of the pyrolysis liquid into a PL and pyrolytic sugar fraction facilitates downstream upgrading, as each fraction can be processed through strategies tailored to their nature and inherent properties.

The chemical composition and properties of PLs are distinctly different from native and other technical lignins [5]. For instance, the high temperatures applied during pyrolysis (typically > 400 °C) cause both thermal depolymerization and recondensation to occur, leading to the formation of new types of bonds, predominantly in the form of inter-unit C–C linkages [6]. As a result, PL fragments are much more stable and difficult to depolymerize, despite their relatively low molecular weight. Catalytic hydrotreatment stands out as one of the most suitable strategies for the upgrading of pyrolytic feedstocks, in which C–C and C–O bond cleavage is assisted by hydrogen addition. Here, unstable unsaturated bonds are hydrogenated and oxygen is removed mainly in the form of water [7]. Previous studies showed the potential of catalytic hydrotreatment for the obtainment of depolymerized mixtures from PLs [8–15] (see Table 1). The majority of the monomers produced from PL are aromatics and alkylphenolics, which are promising compounds due to the possible applications as bulk chemicals, energy carriers and intermediates for the production of biobased materials [16,17].

The (limited) existing literature mainly used PLs obtained from wood (Table 1). It is of high interest to investigate the potential of other

* Corresponding author.
*E-mail address:* h.j.heeres@rug.nl (H.J. Heeres).

https://doi.org/10.1016/j.biombioe.2020.105484
Received 29 June 2019; Received in revised form 12 November 2019; Accepted 24 January 2020
Available online 14 February 2020

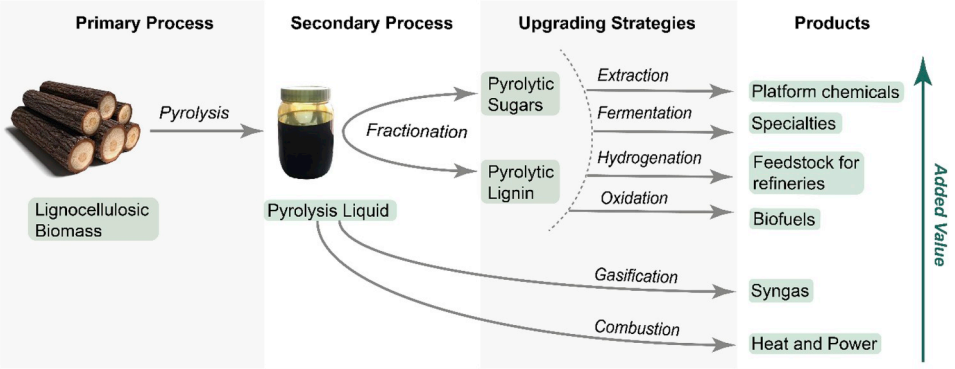


**Fig. 1.** The pyrolysis liquid biorefinery concept.

biomass sources, and compare the performance regarding product yields and particularly the yields of valuable alkylphenolics and aromatics. It is also fundamental to explore agricultural and municipal waste streams, as the use of such feedstocks to generate valuable products represents an important step towards sustainability and the development of a circular economy. Furthermore, a pool of different feeds allows the determination of statistical models to identify correlations between feed characteristics (*e.g.* molecular weight, types of linkages) and predict desired products.

In this research, five pyrolysis liquids produced under similar conditions from different biomass sources (pine, prunings, verge grass, miscanthus and sunflower seed peel) and a commercial pine-derived pyrolysis liquid were subjected to water-fractionation for the obtainment of their respective PLs. The PLs were characterized in detail and hydrotreated with Pd/C at reaction times varying from 1 to 4 h and temperatures in the range of 350–435 °C in the absence of an external solvent. Product properties and the chemical composition of the hydrotreated oils were shown to be highly dependent on the feedstock. The PLs characterization dataset was further used in statistical analyses to support and provide more insights on PL feed-product relations.

## 2. Materials and methods

### 2.1. Chemicals

All pyrolysis liquids were supplied by Biomass Technology Group (BTG, Enschede, the Netherlands). The pyrolysis liquids were produced at 500 °C in a rotating cone reactor [18] (capacity of 5 kg/h, typical residence time < 2 s). The commercial pine-based pyrolysis liquid was produced at 500 °C in a rotating cone reactor [18] (capacity of 5 ton/h) by Empyro B.V. (Hengelo, the Netherlands). The noble-metal catalyst Pd/C was obtained as a powder from Sigma Aldrich and contained 5 wt % of active metal. The average metal nanoparticle size was 2.9 nm (TEM, see Fig. S1) and the surface area was 1025 $m^2/g$ (BET analyses). Nitrogen, hydrogen and helium were obtained from Linde and were all of analytical grade (>99.99% purity). All chemicals in this study were purchased from Sigma-Aldrich and used as received.

### 2.2. Extraction experiments

Pyrolytic lignins (PLs) were obtained by fractionating the pyrolysis liquids with water. The pyrolysis liquid (100 g) was added dropwise to water (150 g) at room temperature under vigorous stirring. The soluble fraction was removed and another portion of water (100 g) was added to the insoluble fraction, followed by vigorous stirring for 10 min and subsequent removal of the soluble fraction. The insoluble fraction was centrifuged for 15 min at 4500 RPM to remove residual water (see Fig. S2 for the detailed scheme). A subsequent fractionation step with dichloromethane (DCM) was applied for characterization purposes, in which 3 g of each PL were mixed with 15 g of DCM and stirred at 1500 RPM for 24 h. The DCM-insolubles were filtered and the DCM-soluble fraction was left overnight to evaporate the solvent.

### 2.3. Feed and product analyses

Hydroxyl content analyses were performed using $^{31}P$ NMR following a procedure described elsewhere [19], using cyclohexanol as the internal standard. $^{31}P$ NMR spectra were acquired on a Bruker NMR spectrometer (600 MHz) at 293 K using a standard 90° pulse, 512 scans and 10 s of relaxation delay. Spectra were processed and analyzed using MestReNova software, refer to the Supplementary Information for details.

Heteronuclear single quantum coherence (HSQC) NMR spectra were acquired on a Bruker NMR spectrometer (600 MHz) with the following parameters: 11 ppm sweep width in the F2 domain ($^1H$), 220 ppm sweep width in the F1 domain ($^{13}C$), 4 scans, 512 increments and a total

**Table 1**
Previous research regarding the catalytic hydrotreatment of PL.

| Biomass source | Temperature (°C) | $H_2$ pressure (bar) | Catalyst(s) used | Solvent used | Monomer yield (wt%) | Ref. |
|---|---|---|---|---|---|---|
| Mixed maple wood | 25–150 | 50 | $Ru/TiO_2$ | Ethanol | 15–16.3[a] | [8] |
| Pine wood | 450 | 100 | Limonite | – | 23.4[b] | [9] |
| Pine wood and forestry residue | 400 | 100 | Ru/C | – | 39.8 and 51.3[b] | [10] |
| Pine wood | 350–400 | 100 | Various (all commercial) | – | 15–33[b] | [11] |
| Hog fuel | 230–415 | 140 | CoMo | – | 50[c] | [12] |
| Maple wood | 340–415 | 1 | HZSM-5 | Tetralin | 22.2–31.3[d] | [13] |
| Rice husk | 260 | 20 | $Ru/ZrO_2$/SBA-15 | Ethanol | – | [14] |
| Pine wood | 340 | 35 | HZSM-5, $\alpha$-$Al_2O_3$, $MoO_3$ | Octane | 3.1–17.1[e] | [15] |

[a] 'Volatile liquids' based on PL intake, obtained from vacuum distillation of the organic product (55 °C, 170 mbar, 1 h).
[b] Monomer yield as determined by GCxGC-FID, based on PL intake.
[c] Fraction of the organic product (≈60-65 wt% of PL intake) boiling within gasoline range, estimated by simulated distillation.
[d] 'Organic distillate' based on PL intake, obtained from vacuum distillation of the organic layer (200 °C, 1.7 mbar, 30 min).
[e] Sum of total hydrocarbons and total phenolics as determined by GC, based on PL intake.

acquisition time of around 1 h. Sample preparation involved the dissolution of 0.15 g of sample in 0.55 g of deuterated dimethyl sulfoxide (DMSO-$d_6$).

$^{13}$C NMR spectra were acquired on a Bruker NMR spectrometer (600 MHz) using a 90° pulse and an inverse-gated decoupling sequence with relaxation delay of 5 s, sweep width of 220 ppm and 2048 scans, with a total acquisition time of 3.5 h and TMS as reference. Sample preparation involved the dissolution of 0.15 g of sample in 0.55 g of DMSO-$d_6$. Spectra were processed and analyzed using MestReNova software, refer to the Supplementary Information for details.

Gel Permeation Chromatography (GPC) analyses were performed using an Agilent HPLC 1100 system equipped with a refractive index detector. Three columns in series of MIXED type E (length 300 mm, i.d. 7.5 mm) were used, with polystyrene as the calibration standard. 0.05 g of the sample was dissolved in 4 mL of tetrahydrofuran (THF) together with 2 drops of toluene as the marker and filtered (filter pore size of 0.2 μm) before analysis.

Thermogravimetric analyses (TGA) were performed using a TGA 7 from PerkinElmer. The samples were heated under a nitrogen atmosphere (nitrogen flow of 50 mL/min), with a heating rate of 10 °C min$^{-1}$ and a temperature ramp of 30–900 °C.

GCxGC-FID analyses were performed on a trace GCxGC system from Interscience equipped with a cryogenic trap and two capillary columns, *i.e.* a RTX-1701 capillary column (30 m × 0.25 mm i.d. and 0.25 μm film thickness) connected by a Meltfit to a Rxi-5Sil MS column (120 cm × 0.15 mm i.d. and 0.15 μm film thickness). Additional information is given in the Supplementary Information.

Elemental analysis (C, H, N) were performed using a EuroVector EA3400 Series CHN–O analyzer with acetanilide as the reference. The oxygen content was determined by difference. All analyses were carried out at least in duplicate and the average value is reported.

The water content was determined by Karl Fischer titration using a Metrohm 702 SM Titrino titration device. About 0.01 g of sample was injected in an isolated glass chamber containing Hydranal (Karl Fischer solvent, Riedel de Haen). The titrations were carried out using the Karl Fischer titrant Composite 5K (Riedel de Haen). All analyses were performed at least 3 times and the average value is reported.

The total organic carbon (TOC) in the water phase was measured by using a Shimadzu TOC-VCSH with an OCT-1 sampler port. Prior to analysis, each sample was diluted around 50 times in water.

The gas phases were analyzed by GC-TCD by using a Hewlett Packard 5890 Series II GC equipped with a Porablot Q $Al_2O_3/Na_2SO_4$ column and a molecular sieve (5 A) column. A reference gas (*i.e.* a mixture containing 55.19% $H_2$, 19.70% $CH_4$, 3.00% CO, 18.10% $CO_2$, 0.51% ethylene, 1.49% ethane, 0.51% propylene and 1.50% propane) was used to identify and quantify the gaseous products.

### 2.4. Data modelling

Principal component analysis (PCA) of the characterization dataset was performed by a routine implemented in Python (version 3.7).

Multivariable regression was used to quantify the effect of PL feed properties on the yield of monomeric alkylphenolics and aromatics (see Equation (1)).

$$Y = a_0 + \sum a_i x_i + \sum a_{ii} x_i^2 + \sum a_{ij} x_i x_j \quad (1)$$

here $x$ is an independent variable, $Y$ is a dependent variable (*i.e.* the yield of monomeric alkylphenolics and aromatics), $a_i$, $a_{ii}$, and $a_{ij}$ are the regression coefficients and $a_0$ is the intercept. The regression coefficients were determined using the Design-Expert (Version 11) software by backward elimination of statistically non-significant parameters. The significant factors were selected based on their $p$-value in the analysis of variance (ANOVA). A parameter with a $p$-value lower than 0.05 is considered significant and thus included in the response model. The variance inflation factor (VIF) was used to identify undesired correlations between the variables. Accordingly, a VIF = 1 implies no correlation at all, and values < 5 relate to moderate (but acceptable) correlations [20]. The leave one out cross validation (LOOCV) of the model was performed by a routine implemented in Python (version 3.7).

### 2.5. Catalytic hydrotreatment experiments

PL was hydrotreated in a 100 mL batch autoclave (Parr, maximum pressure and temperature of 350 bar and 500 °C). The reactor was surrounded by a metal block containing electrical heating elements and channels allowing the flow of cooling water. The reactor content was stirred mechanically at 1000 rpm using a Rushton type turbine with a gas induced impeller. In a typical experiment, the reactor was charged with PL (15 g) and Pd/C (0.75 g, *i.e.* 5 wt% based on PL intake). Subsequently, the reactor was pressurized to 150 bar with hydrogen at room temperature for leak testing, flushed three times and pressurized again to 100 bar. The reactor was heated to the desired temperature at a heating rate of around 10 °C min$^{-1}$, and the reaction time was set at zero when the pre-determined temperature was reached. After the pre-determined reaction time, the reactor was cooled to room temperature at a rate of about 40 °C min$^{-1}$. The final pressure was recorded for mass balance calculations, and the gas phase was sampled in a gas bag for the determination of its composition. The liquid product was collected and weighed. The liquid phase consisted of two layers: an organic layer and an aqueous layer, which were separated by decantation and weighted separately. A small sample of the organic phase was directly taken for GCxGC-FID measurements to ensure that no low molecular weight volatiles were lost in the workup. The solids (*i.e.* catalyst and char) were recovered by first dissolving the organic product and washing the reactor with DCM, then filtering the combined solutions. DCM was removed by overnight evaporation, yielding the final organic product further analyzed. The solids retained in the filter were weighed for char quantification.

## 3. Results and discussion

In the first stage of this research, the water-insoluble PL fraction was extracted from each of the six initial pyrolysis liquids and characterized in detail (section 3.1.). The thus obtained PLs were hydrotreated at different reaction times and temperatures, and the hydrotreated organic phases were analyzed in detail for the identification of feed-product relations (section 3.2.). Finally, the combined yield of aromatics and phenolics after hydrotreatment was selected to build a predictive model based on relevant properties and composition of the PL feed (section 3.3.).

### 3.1. PLs extraction and characterization

The PL fraction of each pyrolysis liquid was obtained by an extraction with water (see experimental section for details). The PL yield for the various biomass sources varied between 30 and 40 wt% (see Fig. S3), except for the product from prunings (PLC), which yielded 62% of PL. Possible explanations of this higher yield are: i) higher amounts of bark, extractives and impurities; ii) higher amounts of polysaccharides covalently bound to the lignin [21]; iii) higher amounts of sugar and/or water molecules trapped during the separation steps, ending up in the insoluble fraction; iv) a combination thereof.

The obtained PLs were then analyzed using a number of techniques to determine relevant macroscopic properties like volatility (TGA) and molecular structure (GPC, NMR, elemental analyses), as well as the amount of monomers initially present (GCxGC-FID). A one-step extraction with DCM was also performed, as the solubility in DCM provides information on the molecular weight (Mw) of the samples [22–24]. An overview of the results is presented in Table 2.

The elemental analysis data show some variability for the H/C and O/C ratios of the PLs, which are expected due to the different biomass

**Table 2**
Characterization results of the PL feeds.

| Property | Pine (PLA) | Commercial Pine (PLB) | Prunings (PLC) | Verge Grass (PLD) | Miscanthus (PLE) | Sunflower seed peel (PLF) |
|---|---|---|---|---|---|---|
| Residual water (wt%) | 7.5 | 8.2 | 11.2 | 7.6 | 7.6 | 7.6 |
| Elemental composition (wt%, dry basis) | | | | | | |
| C | 67.9 | 65.4 | 66.5 | 64.3 | 65.7 | 67.5 |
| H | 6.5 | 6.6 | 6.6 | 6.8 | 6.4 | 6.6 |
| O | 25.6 | 28 | 25.4 | 27.3 | 27.7 | 24.5 |
| N | <0.1 | <0.1 | 1.5 | 1.6 | 0.2 | 1.4 |
| H/C (molar) | 1.15 | 1.21 | 1.19 | 1.27 | 1.17 | 1.16 |
| O/C (molar) | 0.28 | 0.32 | 0.28 | 0.31 | 0.31 | 0.27 |
| Average Mw (g/mol) | 741 | 690 | 662 | 713 | 668 | 757 |
| DCM insolubles (wt%) | 34.3 | 30.3 | 53.4 | 63.7 | 34.4 | 59.4 |
| TGA residue (wt%)[a] | 19.8 | 17.3 | 23.3 | 26.1 | 20.4 | 26.5 |
| Monomers (wt%)[b] | 12.8 | 12.5 | 10.9 | 10.1 | 14.1 | 12.1 |
| Aliphatic C (area%)[c] | 23.3 | 20.7 | 26.9 | 31.3 | 20.4 | 26.4 |
| MeO-Ar (area%)[c] | 6.1 | 7.7 | 5.5 | 5.4 | 7.8 | 6.4 |
| Aliphatic C–O (area%)[c] | 17.5 | 16.0 | 16.5 | 17.5 | 14.6 | 13.7 |
| Aromatic C–H (area%)[c] | 30.2 | 31.9 | 28.8 | 24.3 | 32.5 | 30.6 |
| Aromatic C–C (area%)[c] | 15.6 | 15.8 | 16.1 | 15.6 | 17.3 | 16.2 |
| Aromatic C–O (area%)[c] | 7.2 | 7.8 | 6.2 | 5.9 | 7.4 | 6.7 |
| Aliphatic OH (mmol/g PL)[d] | 1.87 | 1.73 | 0.98 | 1.03 | 1.56 | 1.18 |
| Condensed OH (mmol/g PL)[d] | 0.36 | 0.57 | 0.05 | 0.06 | 0.39 | 0.09 |
| S-unit OH (mmol/g PL)[d] | 0.00 | 0.00 | 0.00 | 0.00 | 0.67 | 0.19 |
| G-unit OH (mmol/g PL)[d] | 2.11 | 2.08 | 0.05 | 0.06 | 1.42 | 0.83 |
| Phenolic OH (mmol/g PL)[d] | 1.00 | 0.74 | 0.05 | 0.08 | 1.44 | 0.58 |
| Acid OH (mmol/g PL)[d] | 0.12 | 0.08 | 0.00 | 0.00 | 0.18 | 0.06 |

[a] TGA residue at T = 900 °C.
[b] Integration results of the GCxGC-FID chromatograms.
[c] Integration results of the $^{13}$C NMR spectra.
[d] Integration results of the $^{31}$P NMR spectra. S-unit OH refers to the phenolic OH of an S unit (two methoxy side groups); G-unit OH refers to the phenolic OH of a G unit (one methoxy side group); Phenolic OH refers to non-methoxylated unit; Condensed OH refers to C5-substituted and/or condensed phenolics.

sources used. The observed values are in line with literature data, which reported H/C and O/C ratios varying between 1.0 and 1.3 (H/C) and 0.25–0.4 (O/C) for PLs [11]. In detail, PLD shows the highest H/C molar ratio, *i.e.* a more aliphatic character. The nitrogen content of the PLs are between <0.1 and 1.6 wt%, and are below the detection limit for PLA, PLB and PLE, while significant for PLC, PLD and PLF. This is an important parameter to consider in the subsequent catalytic hydrotreatment step as studies have demonstrated a negative effect of nitrogen on hydroprocessing reactions due to catalyst poisoning [25].

Thermogravimetric analyses (TGA) were performed to evaluate the volatility of the different PLs. The weight loss profiles of the PLs can be divided into three main stages: *i)* volatilization of residual water and low MW molecules (<160 °C); *ii)* release of phenolic monomers and thermal cracking of lignin fragments with extensive formation of volatiles (160–500 °C); *iii)* further pyrolysis and carbonization (500–800 °C), in line with literature data [26]. TGA analyses also provide information on the amount of non-volatiles by considering the residue at 900 °C. The amount of residue was lower for PLA, PLB and PLE when compared to PLC, PLD and PLF. High residues are either the result of larger fragments/impurities initially present or higher amounts of thermally unstable fragments that repolymerise during TGA analysis. Interestingly, the DCM fractionation resulted in a similar grouping, *i.e.* PLA, PLB and PLE presented much lower DCM insolubles in comparison with PLC, PLD and PLF (see Fig. S4). While solubility in DCM is considered to be related to Mw (see Figs. S5 and S6), comparative GPC analyses of the PLs surprisingly did not show significant differences in their average molecular weight (Mw), see Figs. S7 and S8. This suggests that other characteristics besides Mw, such as differences in chemical composition, have a higher impact on the DCM solubility than the Mw.

The monomeric fractions present in the PLs were categorized and quantified through GCxGC-FID using established procedures [9,10,22]. The total amount of monomers did not vary significantly among the PLs

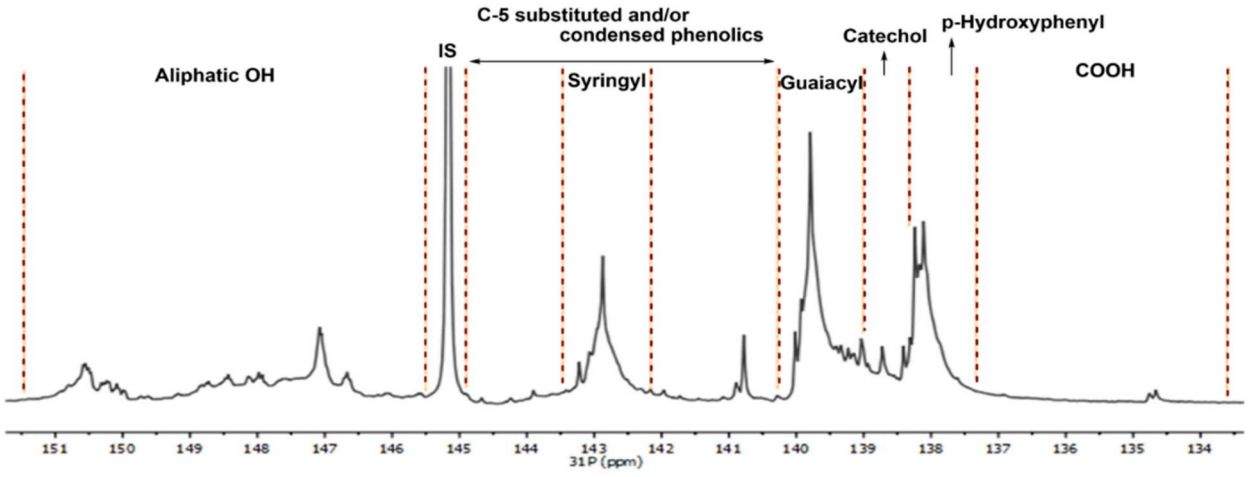


**Fig. 2.** Representative $^{31}$P NMR spectrum of a PL.

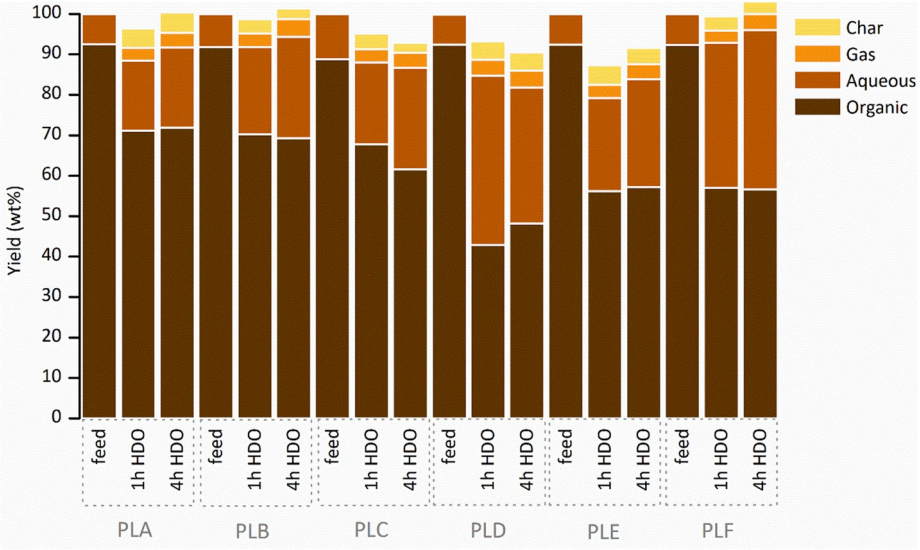


**Fig. 3.** Mass balances of the reactions performed at 350 °C.

(*i.e.* between 10 wt% and 14 wt%, see Fig. S9), but PLC and PLD showed a relatively lower amount of alkylphenolics. Further NMR analyses provided structural information on a molecular level for the non-volatile fragments (*i.e.* non-GC detectables), which are the major fraction in the PLs. For instance, the distribution of $^{13}$C NMR relative areas indicated the presence of (oxygenated) aliphatics (from extractives, residual sugars and aromatic side groups) and aromatic linkages (from lignin itself) within all PLs (see Fig. S10). Furthermore, it showed variations mostly in the amount of aliphatic C–H and aromatic C–H bonds. In line with the GCxGC results, PLC and PLD presented lower amounts of aromatic carbons, together with a higher amount of aliphatic carbons. The reasons behind such differences may be related to the biomass source (*i.e.* higher fatty acid content) and/or to the presence of impurities. It also suggests that for complex biomass mixtures (such as the prunings and grasses used for obtaining PLC and PLD), extra fractionation steps might be necessary in order to increase the proportion of aromatics in the PL fraction.

$^{31}$P NMR analyses provided detailed information on the content and distribution of the hydroxy groups present within the PLs structure, and showed quite large variations among the PLs (see Fig. S11). For instance, PLA, PLB and PLE have a relatively high concentration of OH groups. As PLA and PLB are both derived from pine, the aromatic fraction is guaiacyl-based [9], while PLE (from miscanthus) also contains syringyl units [27]. PLF presented an intermediate level of hydroxylated aromatics, while both PLC and PLD have a very low and mostly aliphatic OH content. A representative $^{31}$P NMR spectrum is shown in Fig. 2.

The PL characterization dataset as given in Table 2 was further used for a PCA analysis, which allowed its projection in a 2D score-plot while retaining most of the information (see Fig. S12). For instance, 79.4% of the data variance was retained in the first two principal components, with the principal component 1 (PC1) accounting for 63.2% of the variance. PCA shows two main clusters separated by PC1 (*i.e.* PLA, PLB, PLE and PLC, PLD, PLF), confirming the structural similarities among the PLs within each cluster (as found by the analyses performed, *vide supra*).

### 3.2. Catalytic hydrotreatment of the PLs

All six PLs were hydrotreated at 350 °C for 1 h and 4 h with Pd/C as the catalyst. The catalyst was selected based on a previous screening study performed with pine-derived PL [11]. After the reactions, a biphasic liquid product was obtained, consisting of a dark organic phase (here referred as *hydrotreated organic phase*) and an aqueous phase. Accordingly, water formation is an indicative of the occurrence of hydrodeoxygenation reactions. Hydrotreated organic phases were obtained in yields varying from 42.9% up to 71.9 wt%, and char and gas phases together accounted for <10 wt% of the products, regardless of the feedstock (see Fig. 3 and Table S3). The low amounts of char and gas are highly desirable to minimize carbon losses. Furthermore, the increase in reaction time from 1 h to 4 h did not change the product distribution substantially, suggesting that the majority of the deoxygenation reactions occur within a time scale of 1 h. This observation is in line with a previous hydrotreatment study, which showed that deoxygenation and depolymerization of Alcell lignin takes place already when heating up the samples to elevated temperatures [28]. The hydrogen consumption for the 1 h hydrotreatment reaction varied between 285 and 336 nL $H_2$/kg PL and increased for the 4 h reaction (342–398 nL $H_2$/kg PL, see Table S3). Besides showing that the PL biomass source has a significant impact on the hydrogen consumption during upgrading, it clearly shows that other reaction pathways than deoxygenation take place at longer reaction times. For instance, hydrogen can be consumed in a range of reactions besides deoxygenation, *i.e.* hydrocracking, hydrogenation, hydrogenolysis, demethoxylation [7].

The hydrotreated organic phases contained large amounts of carbon (>77 wt% on dry basis) and limited amounts of water (1.1–5.3 wt%). The oxygen contents of the hydrotreated organic phases were considerably lower than for the starting material, with the largest oxygen reduction for PLF (*i.e.* 1.5 wt%). Good mass balance closures of at least 87.3% were achieved for all the experiments. Carbon yields of the hydrotreated organic phases varied largely between 54.1 and 94.3 wt% (based on the carbon content of each PL feed), indicating that carbon losses to the gas, char and aqueous phases (in the form of small polar compounds) occur, and that the extent depends on the PL source. The hydrotreated organic phases from the PLs derived from pine wood (*i.e.* PLA and PLB) presented the overall highest oil and carbon yields (see Table S4 for the results in detail).

The three PLs that yielded more aromatics and alkylphenolics after a hydrotreatment for 4 h and 350 °C (*i.e.* PLA, PLB and PLF, *vide infra*) were also hydrotreated at 400 °C. The products from reactions performed at 400 °C were less viscous than the products from reactions performed at 350 °C, and a slight decrease in the organic yield is observed, together with slightly higher amounts of gas and aqueous phases (see Fig. S13). Accordingly, higher temperatures increase the overall reaction rates and thus hydrogen consumption (see Table S3), so more oxygen is removed as water, more gaseous products are formed

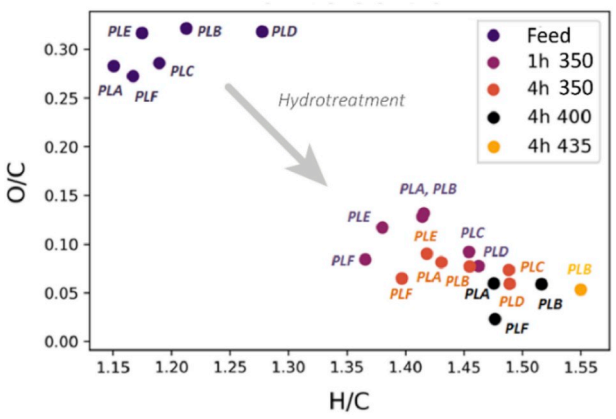


**Fig. 4.** Van Krevelen plot of the PLs and their hydrotreated organic phases.

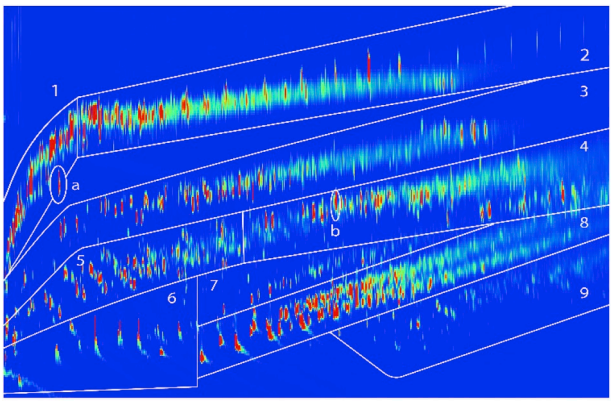


**Fig. 5.** Representative GCxGC-FID chromatogram of a hydrotreated organic phase from PLB (4 h, 400 °C). 1 = cyclic alkanes, 2 = linear/branched alkanes, 3 = aromatics, 4 = naphtalenes and polycyclic aromatic hydrocarbons, 5 = ketones/alcohols, 6 = acids, 7 = guaiacols, 8 = alkylphenolics, 9 = catechols. a = internal standard and b = BHT (stabilizer in THF).

and the final oil has a lower viscosity due to enhanced hydrocracking. This is in line with previous pyrolysis liquids hydroprocessing literature [24,29,30]. PLB was used as reference and additionally hydrotreated at 435 °C. This led to high carbon losses to char (10 wt%) and gas (8.1%), with no substantial improvements in the oil properties and monomer yields (*vide infra*). These findings suggest that the catalytic hydrotreatment of PL is best performed at intermediate temperatures (350–400 °C) which results in good deoxygenation and hydrocracking rates without excessive gas and solid formation.

### 3.3. Products composition and properties

#### 3.3.1. Gas phase analysis

Despite the low amounts of gas produced, their composition was assessed through gas chromatography. At least 67 mol% of the gas phase corresponded to $H_2$, indicating that all reactions were carried using an excess of hydrogen (see Fig. S14). The hydrogen amount in the gas phase decreased at longer reaction times and higher temperatures due to the higher rates of hydro (deoxy)genation and hydrocracking reactions. The main gaseous products were CO, $CO_2$, $CH_4$ and $C_2$–$C_3$ hydrocarbons. The hydrocarbons are likely formed by hydrocracking reactions, whereas $CO_2$ and CO are the result of (acid-catalyzed) decarboxylation and decarbonylation reactions. CO can be also derived from the reverse water-gas shift (RWGS) reaction. Methane ($CH_4$) is produced by methanation of CO and $CO_2$, as well as by the direct hydrogenolysis of methoxy substituents present on the PL aromatic network. PLC and PLD products showed a relatively low concentration of methane, in line with the lower amount of methoxyphenols in these samples.

#### 3.3.2. Composition of the hydrotreated organic phase

The hydrotreated organic phases were characterized in detail by elemental analysis, GCxGC-FID, TGA, GPC and NMR techniques. The elemental composition of the PLs and their hydrotreated organic phases are illustrated in the form of a van Krevelen plot (see Fig. 4).

It is clear that the hydrotreated samples have a higher H/C and a lower O/C ratio than the PL feeds, indicating the occurrence of hydrogenation and hydrodeoxygenation reactions. The results from elemental analysis also support that extensive deoxygenation already happens in the first hour of reaction, as the O/C ratios of the 1 h hydrotreated organic phases are significantly lower than the O/C ratios of their PL feeds. This is in line with the large amounts of water observed in the 1 h product mixtures (*vide supra*). When extending the batch time from 1 to 4 h at 350 °C and increasing the temperature from 4 h at 350 °C to 400 °C, the H/C ratio increase whereas the O/C ration decrease, indicating a higher hydro (deoxy)genation and hydrocracking activity. The 435 °C data point (PLB) suggests that a higher temperature leads to over-reduction (*e.g.* from aromatics to cycloalkanes) and cracking reactions, as the O/C ratio did not change significantly whereas the H/C ratio increased considerably. The H/C and O/C molar ratios of the hydrotreated organic phases in the van Krevelen plot are located between those of typical monomeric alkylphenolics and aromatics [31].

GCxGC-FID analyses were performed to identify and quantify the various classes of monomeric products present in the hydrotreated organic phases. Established procedures [9,10,23] were used and a representative chromatogram is shown in Fig. 5.

Summarized integration results for the PLs and their hydrotreated organic phases are shown in Fig. 6. The main group of GCxGC-FID detectables were alkylphenolics (which include catechols and guaiacols), followed by aromatics (which include naphtalenes) (cyclo)alkanes (*i.e.* cyclic alkanes and alkanes), and polar monomers (*i.e.* acids and ketones). The main monomeric species detected by GC/MS-FID are listed in Table S5.

After 1 h of hydrotreatment, monomer yields varied considerably among the PLs, *i.e.* from 13 to 23 wt% based on the hydrotreated organic phase. A longer reaction time led to an increase in the amounts of monomers, and the pyrolytic lignins from pine (PLA and PLB) showed the highest values. The combined yield of alkylphenolics and aromatics was highest for PLA, PLB and PLF. As such, these were also hydrotreated at 400 °C instead of 350 °C. This gave a large impact on the monomer yields, which doubled to around 60 wt% on the hydrotreated organic phase, corresponding to 39.1 wt% (PLA), 38.8 wt% (PLB) and 37.4 wt% (PLF) based on PL intake. Besides the formation of higher amounts of alkylphenolics and aromatics, undesired over-reduction to cycloalkanes also occurred to a significant extent. PLB was also hydrotreated at 435 °C, and despite the slightly higher monomer yields on the organic product, it corresponded to only 31.5 wt% based on PL intake due to lower oils yields as a result of extensive gas and char formation during hydrotreatment. In addition, the amounts of over-reduced products (cycloalkanes) further increased. These findings are in line with the elemental analysis results, with higher temperatures giving products with a higher H/C ratio (*vide supra*).

The maximum amount of monomers detected by GCxGC-FID was of 60 wt% based on hydrotreated organic phase, indicating that the products also contain higher molecular weight, non-GC detectables. This was confirmed by performing GPC analyses on the hydrotreated organic phases and the starting PLs. A representative GPC curve of PLB is shown in Fig. 7. Clearly, the Mw of the hydrotreated organic phases are significantly lower when compared to their feed, indicating that substantial depolymerization occurs during the catalytic hydrotreatment. Mw are a strong function of the hydrotreatment temperature (see also Figures S15, S16 and S17), with higher temperatures leading to lower Mw. These results are in line with the PCA clustering observed in section 4 (*vide infra*).

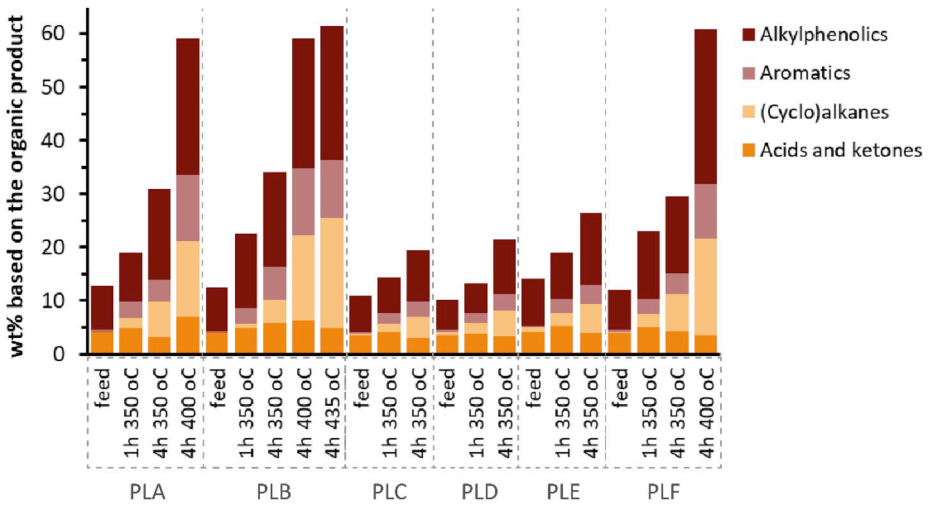


**Fig. 6.** GCxGC-FID results for the PL feeds and corresponding hydrotreated product phases .

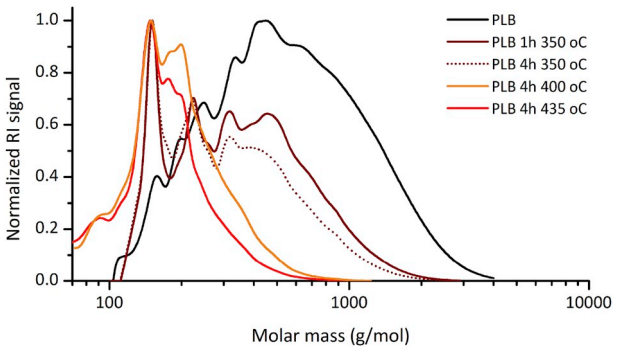


**Fig. 7.** Representative GPC curves for PLB and its hydrotreated products.

Representative TG and dTG curves of PLB and its hydrotreated products are given in Fig. S18. Overall, the samples became more volatile after hydrotreatment, though the volatility is strongly affected by the PL source and hydrotreatment conditions. Already after the 1 h hydrotreatment reactions at 350 °C, the TGA residue was substantially lower for all PLs, yet particularly for PLA, PLB and PLE (see Fig. S19). Longer reaction times as well as higher temperatures resulted in higher volatilities due to more extensive cracking of the oligomeric structures. For PLA, PLB and PLF, all volatiles were released at TGA temperatures below 300 °C (see Fig. S20).

Further structural changes during the hydrotreatment reaction, especially regarding the non-volatile PL fragments, were accessed by NMR. A typical NMR HSQC spectrum of a PL can be divided in three main areas, *i.e.* aliphatics (from alkyl groups), oxygenated aliphatics (from methoxy side groups, residual sugars and extractives) and

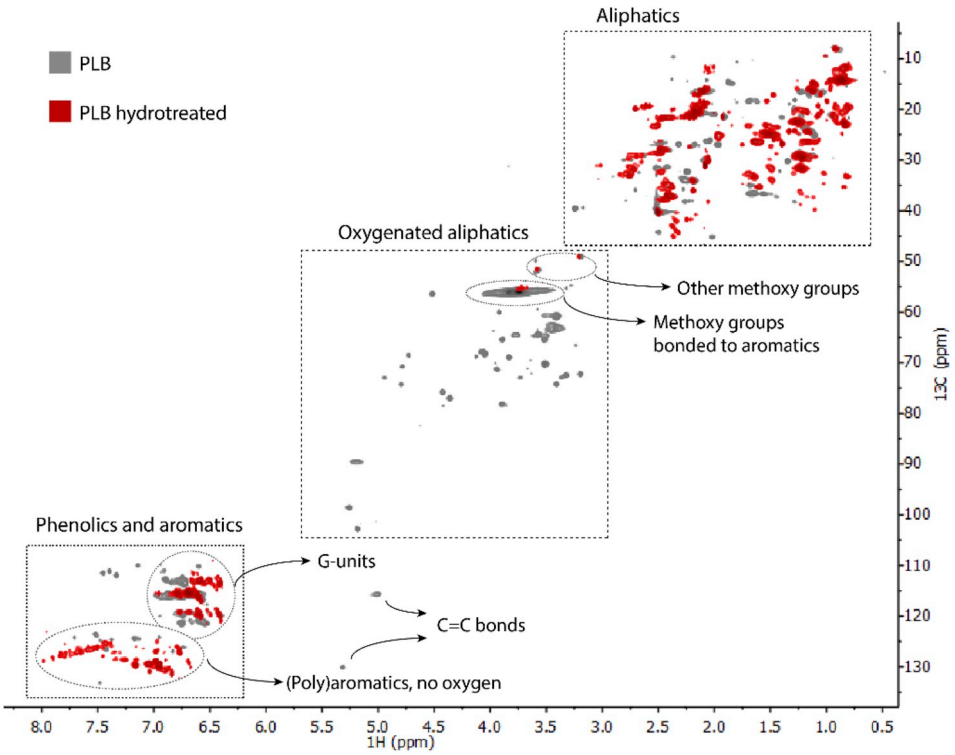


**Fig. 8.** NMR HSQC spectra of PLB and its hydrotreated product (4 h, 400 °C).

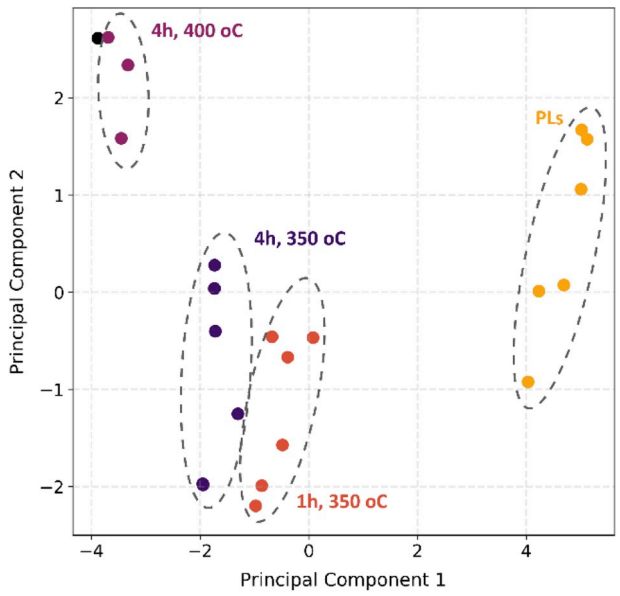


**Fig. 9.** Score plot (PC1 = 71.7% and PC2 = 17.7% of the dataset variance) of all PLs and their hydrotreated organic phases.

aromatics (from lignin). The main structural changes occurring during hydrotreatment are illustrated in Fig. 8. For instance, the area related to oxygenated aliphatic bonds is greatly affected, and resonances are nearly absent after reaction. The intensity of the peaks in the aromatics and aliphatics area increases significantly after hydrotreatment due to hydrodeoxygenation reactions. While the aromatic area in PL is mostly comprised of guaiacyl units (in the case of pine), a new region related to deoxygenated (poly)aromatics is observed in the hydrotreated organic phase.

$^{13}$C NMR analyses showed similar trends of structural changes for all PLs (see Fig. S21 for PLB representative results). By integrating the relative areas, information about the reactivity of certain components is obtained. For instance, the intensity of the aliphatic C–H bonds increases initially, but then decreases with higher reaction time and temperature. This is likely due to the loss of small hydrocarbons to the gas phase. However, at even higher severity (higher temperatures, longer batch times) the intensity increases again, likely due to over-reduction of aromatic rings and the formation of cycloalkanes. The aliphatic C–O bonds, aromatic C–O bonds and methoxy groups decrease substantially due to deoxygenation. Additional $^{31}$P NMR analyses were performed with PLB and its hydrotreated organic phase, revealing that the absolute concentration of aromatic OH was about constant (see Fig. S22). Its distribution, however, shifted from guaiacyl units to mostly phenolics, while the proportion of aliphatic OH groups decreased. This interesting result suggests that most of the oxygen removed during the hydrotreatment originates from methoxy side groups and other ether bonds present within the PL structure (*e.g.* diaryl ether linkages [32]), rather than phenolic groups.

## 4. PCA analysis

A large dataset was obtained from the characterization of the six PL feeds and their respective hydrotreated products. A PCA analysis was applied to visualize trends and clusters. The first two principal components together retained 89.4% of the data variance (*i.e.* PC1 = 71.7% and PC2 = 17.7%), allowing a reliable visualization of the dataset in a 2D score-plot (see Fig. 9 and Fig. S23 for the variables' loadings of PC1 and PC2). For instance, four clusters are clearly visible, and each one is related to a set of conditions: *i)* PL feeds, *ii)* hydrotreated organic phases – 1 h at 350 °C, *iii)* hydrotreated organic phases – 4 h at 350 °C and *iv)* hydrotreated organic phases – 4 h at 400 °C. This clear clustering

**Table 3**
Model summary.

| Source | p-value | VIF | $R^2$ | Adj $R^2$ | Pred $R^2$ |
|---|---|---|---|---|---|
| Model | 0.0083 | – | 0.9944 | 0.9861 | 0.9464 |
| Var1- Avg Mw | 0.0523 | 1.27 | | | |
| Var2- Arom C–C | 0.0374 | 1.37 | | | |
| Var3- Arom C–O | 0.0031 | 1.09 | | | |

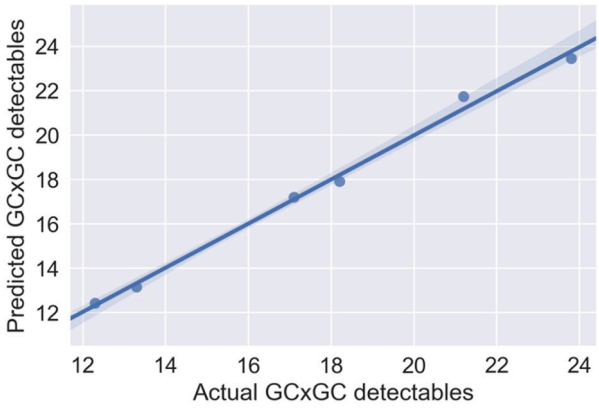


**Fig. 10.** Model prediction of monomeric aromatics and alkylphenolics ($R^2$ = 0.9944).

indicates that already after short 1 h hydrotreatment, the hydrotreated product properties differ considerably from the initial PLs. In addition, within each cluster, a spread in data points is also observed, revealing that the PL feed plays a role. Furthermore, the time effect seems relatively limited as the cluster with datapoints from PLs hydrotreated at 350 °C for 1 h is in close proximity with the cluster of PLs hydrotreated at 350 °C for 4 h. However, the position of the cluster of hydrotreated product oils obtained at 350 °C for 4 h within the graph is far from the cluster obtained for the same oil at 400 °C and 4 h, which clearly indicates that the reaction temperature has a by far higher impact on the product properties than reaction time. Thus, it can be concluded from the PCA analyses that the PL feed as well as the process conditions and particularly temperature impact the properties of the hydrotreated product oils.

## 5. Statistical modelling

Regression analyses were performed to determine quantitative relations between the properties of the PLs (*vide supra*, Table 2) and the combined yield of monomeric aromatics and alkylphenolics in the product oils after hydrotreatment. The latter was selected as these are the preferred products based on volume and product prices. The dataset obtained at 4 h and 350 °C were used as all (six) PLs were hydrotreated at such conditions (see Fig. S24 for the correlation matrix containing all variables).

Analyses of the data using Design Expert software gave a surprisingly simple linear model for the yield of aromatics and alkylphenolics, with only three PL properties as input, *i.e.* the average Mw (from GPC analysis) and relative areas of the aromatic C–C and C–O bonds (from $^{13}$C NMR analysis). A summary of the model is presented in Table 3 and the model equation is given in Equation (2). This equation is based on the following data ranges: 668–757 g/mol (Avg Mw), 15.6–17.3% relative area (Arom C–C), 5.9–7.8% relative area (Arom C–O) and 7.8–26 wt% (combined yield of monomeric aromatics and alkylphenolics after hydrotreatment).

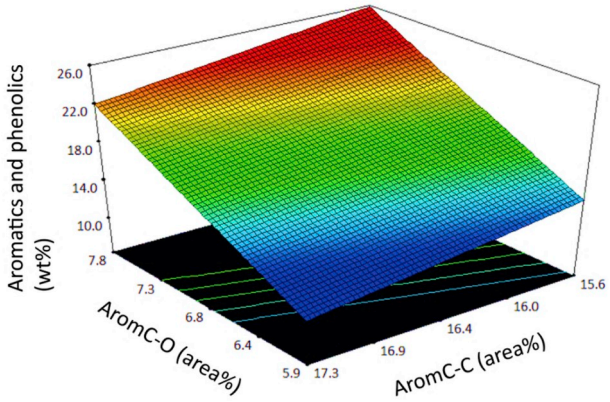


**Fig. 11.** Surface plot of the model (aromatic and alkylphenolic yields *versus* linkages in the PL feed).

$$GCxGC_{(Aromatics+Phenolics)} = -8.97707 + 0.028543 * Avg\ MW - 2.15461 * AromC - C + 5.99713 * AromC - O \quad (2)$$

The p-value of each term is below 0.05, indicating that all are statistically significant. The VIF is below 1.3, indicating that the variables are not strongly correlated. The high $R^2$ value indicates that the model describes the experimental data very well, which is also clear from the parity plot given in Fig. 10. The adjusted $R^2$ and predicted $R^2$, known to be better model indicators than the $R^2$ value, also are high, suggesting no significant overfitting or the use of redundant variables in the model. The residuals (*i.e.* difference between observed and predicted values) were also evaluated, as by definition they should be independent from the response variables (*i.e.* randomly distributed). This was indeed observed in the plots shown in Fig. S25.

A leave one out cross validation (LOOCV) was applied to verify the generalizability of the model outside the original dataset. The LOOCV uses a single datapoint as the validation data, and the remaining observations as the training data. This process is repeated until each datapoint is used once for validation [33]. The LOOCV model showed a very good fit as well ($R^2$ = 0.9326, see Fig. S26), indicating a good predictive capacity when using new datapoints.

The 3D surface shown in Fig. 11 illustrates the aromatics and alkylphenolics yields as a function of the aromatic C–O and aromatic C–C $^{13}$C NMR relative areas, which have a large impact on the monomer yields (see Equation (2)). It clearly shows that the monomer yield after hydrotreatment is higher when the PL feed contains a higher amount of aromatic C–O bonds and a lower amount of aromatic C–C bonds. This may be explained by assuming that C–O bonds are relatively easier to cleave during hydroprocessing than C–C bonds, in line with literature data on lignin and PL model components [9]. To the best of our knowledge, this is the first attempt to obtain relations between PL feed properties and monomer yield data. The simple model here disclosed can be useful for future selection of PL feeds for catalytic hydrotreatment, aiming at high yields of aromatics and alkylphenolics.

## 6. Conclusions

The catalytic hydrotreatment of six well-characterized PLs from different biomass sources was investigated under a range of conditions. The best results were achieved with pine derived PLs, which favored high oil yields (up to 71.9 wt%) and monomer yields (up to 39.1 wt% based on PL intake), as well as low gas and char formation. The PL feed is shown to have a significant impact on the oil quality, product distribution and yields of valuable monomers (*i.e.* aromatics and alkylphenolics). The different PLs were characterized in detail and, together with the hydrotreatment data, used to generate a model able to predict the combined yield of monomeric aromatics and alkylphenolics in the organic phase after catalytic hydrotreatment. It was shown that particularly the average Mw (from GPC analysis) and relative areas of aromatic C–C and aromatic C–O bonds (from $^{13}$C NMR analysis) have a major effect. We expect this model to be of use in future selections of PL feeds when envisioning high yields of aromatics and alkylphenolics via catalytic hydrotreatment.

## Acknowledgements

Financial support from the Science without Borders program (Brazil) is gratefully acknowledged. The TKI Biobased Economy and the Netherlands Enterprise Agency (RVO) are gratefully acknowledged for their financial support of the Lignin2Fuel project under agreement no. TEBE116143. We also thank Erwin Wilbers, Marcel de Vries, Léon Rohrbach, Jan Henk Marsman and Anne Appeldoorn for their technical support and BTG for supplying the pyrolysis liquids. Hans van der Velde is acknowledged for performing the elemental analysis.

## Appendix A. Supplementary data

Supplementary data to this article can be found online at https://doi.org/10.1016/j.biombioe.2020.105484.

## References

[1] S. Czernik, A. Bridgwater, Overview of applications of biomass fast pyrolysis oil, Energy Fuels 18 (2004) 590–598, https://doi.org/10.1021/ef034067u.
[2] A.V. Bridgwater, Upgrading biomass fast pyrolysis liquids, Environ. Prog. Sustain. Energy 31 (2012) 261–268, https://doi.org/10.1002/ep.11635.
[3] A. Oasmaa, E. Kuoppala, Y. Solantausta, Fast pyrolysis of forestry residue. 2. Physicochemical composition of product liquid, Energy Fuels 17 (2003) 433–443, https://doi.org/10.1021/ef020206g.
[4] F. Cherubini, The biorefinery concept: using biomass instead of oil for producing energy and chemicals, Energy Convers. Manag. 51 (2010) 1412–1421, https://doi.org/10.1016/j.enconman.2010.01.015.
[5] J. Rencoret, G. Marques, A. Gutiérrez, D. Ibarra, J. Li, G. Gellerstedt, J.I. Santos, J. Jiménez-Barbero, Á.T. Martínez, J.C. del Río, Structural characterization of milled wood lignins from different eucalypt species, Holzforschung 62 (2008), https://doi.org/10.1515/HF.2008.096.
[6] R. Bayerbach, D. Meier, Characterization of the water-insoluble fraction from fast pyrolysis liquids (pyrolytic lignin). Part IV: structure elucidation of oligomeric molecules, J. Anal. Appl. Pyrolysis 85 (2009) 98–107, https://doi.org/10.1016/j.jaap.2008.10.021.
[7] A.H. Zacher, M.V. Olarte, D.M. Santosa, D.C. Elliott, S.B. Jones, A review and perspective of recent bio-oil hydrotreating research, Green Chem. 16 (2014) 491–515, https://doi.org/10.1039/C3GC41382A.
[8] W. Chen, D.J. McClelland, A. Azarpira, J. Ralph, Z. Luo, G.W. Huber, Low temperature hydrogenation of pyrolytic lignin over Ru/TiO 2: 2D HSQC and 13 C NMR study of reactants and products, Green Chem. 18 (2016) 271–281, https://doi.org/10.1039/C5GC02286J.
[9] I. Hita, H.J. Heeres, P.J. Deuss, Insight into structure–reactivity relationships for the iron-catalyzed hydrotreatment of technical lignins, Bioresour. Technol. 267 (2018) 93–101, https://doi.org/10.1016/j.biortech.2018.07.028.
[10] A. Kloekhorst, J. Wildschut, H. Jan Heeres, Catalytic hydrotreatment of pyrolytic lignins to give alkylphenolics and aromatics using a supported Ru catalyst, Catalysis Science & Technology 4 (2014) 2367–2377, https://doi.org/10.1039/C4CY00242C.
[11] M.B. Figueirêdo, Z. Jotic, P.J. Deuss, R.H. Venderbosch, H.J. Heeres, Hydrotreatment of pyrolytic lignins to aromatics and phenolics using heterogeneous catalysts, Fuel Process. Technol. 189 (2019) 28–38, https://doi.org/10.1016/j.fuproc.2019.02.020.
[12] J. Piskorz, P. Majerski, D. Radlein, D. Scott, Conversion of lignins to hydrocarbon fuels, Energy Fuels 3 (1989) 723–726, https://doi.org/10.1021/ef00018a011.
[13] R. Sharma, N. Bakhshi, Upgrading of pyrolytic lignin fraction of fast pyrolysis oil to hydrocarbon fuels over HZSM-5 in a dual reactor system, Fuel Process. Technol. 35 (1993) 201–218, https://doi.org/10.1016/0378-3820(93)90099-P.
[14] Z. Tang, Y. Zhang, Q. Guo, Catalytic hydrocracking of pyrolytic lignin to liquid fuel in supercritical ethanol, Ind. Eng. Chem. Res. 49 (2010) 2040–2046, https://doi.org/10.1021/ie9015842.
[15] X. Zhang, Q. Chen, Q. Zhang, C. Wang, L. Ma, Y. Xu, Conversion of pyrolytic lignin to aromatic hydrocarbons by hydrocracking over pristine MoO3 catalyst, J. Anal. Appl. Pyrol. 135 (2018) 60–66, https://doi.org/10.1016/j.jaap.2018.09.020.
[16] J.H. Lora, Lignin: a platform for renewable aromatic polymeric materials, in: P.C. K. Lau (Ed.), Quality Living through Chemurgy and Green Chemistry, Springer Berlin Heidelberg, Berlin, Heidelberg, 2016, pp. 221–261, https://doi.org/10.1007/978-3-662-53704-6_9.

[17] J. Zakzeski, P.C. Bruijnincx, A.L. Jongerius, B.M. Weckhuysen, The catalytic valorization of lignin for the production of renewable chemicals, Chem. Rev. 110 (2010) 3552–3599, https://doi.org/10.1021/cr900354u.
[18] B.M. Wagenaar, W. Prins, W.P.M. van Swaaij, Pyrolysis of biomass in the rotating cone reactor: modelling and experimental justification, Chem. Eng. Sci. 49 (1994) 5109–5126, https://doi.org/10.1016/0009-2509(94)00392-0.
[19] S. Constant, H.L.J. Wienk, A.E. Frissen, P. de Peinder, R. Boelens, D.S. van Es, R.J. H. Grisel, B.M. Weckhuysen, W.J.J. Huijgen, R.J.A. Gosselink, P.C.A. Bruijnincx, New insights into the structure and composition of technical lignins: a comparative characterisation study, Green Chem. 18 (2016) 2651–2665, https://doi.org/10.1039/C5GC03043A.
[20] E.R. Mansfield, B.P. Helms, Detecting multicollinearity, Am. Statistician 36 (1982) 158–160, https://doi.org/10.1080/00031305.1982.10482818.
[21] H. Nishimura, A. Kamiya, T. Nagata, M. Katahira, T. Watanabe, Direct evidence for α ether linkage between lignin and carbohydrates in wood cell walls, Sci. Rep. 8 (2018) 6538, https://doi.org/10.1038/s41598-018-24328-9.
[22] I. Hita, P.J. Deuss, G. Bonura, F. Frusteri, H.J. Heeres, Biobased chemicals from the catalytic depolymerization of Kraft lignin using supported noble metal-based catalysts, Fuel Process. Technol. 179 (2018) 143–153, https://doi.org/10.1016/j.fuproc.2018.06.018.
[23] S. Agarwal, R.K. Chowdari, I. Hita, H.J. Heeres, Experimental studies on the hydrotreatment of kraft lignin to aromatics and alkylphenolics using economically viable Fe-based catalysts, ACS Sustain. Chem. Eng. 5 (2017) 2668–2678, https://doi.org/10.1021/acssuschemeng.6b03012.
[24] R. Venderbosch, A. Ardiyanti, J. Wildschut, A. Oasmaa, H. Heeres, Stabilization of biomass-derived pyrolysis oils, J. Chem. Technol. Biotechnol. 85 (2010) 674–686, https://doi.org/10.1002/jctb.2354.
[25] E. Furimsky, F.E. Massoth, Deactivation of hydroprocessing catalysts, Catal. Today 52 (1999) 381–495.
[26] S. Wang, H. Lin, B. Ru, W. Sun, Y. Wang, Z. Luo, Comparison of the pyrolysis behavior of pyrolytic lignin and milled wood lignin by using TG–FTIR analysis, J. Anal. Appl. Pyrol. 108 (2014) 78–85, https://doi.org/10.1016/j.jaap.2014.05.014.
[27] R. El Hage, N. Brosse, L. Chrusciel, C. Sanchez, P. Sannigrahi, A. Ragauskas, Characterization of milled wood lignin and ethanol organosolv lignin from miscanthus, Polym. Degrad. Stabil. 94 (2009) 1632–1638, https://doi.org/10.1016/j.polymdegradstab.2009.07.007.
[28] A. Kloekhorst, H.J. Heeres, Catalytic hydrotreatment of Alcell lignin using supported Ru, Pd, and Cu catalysts, ACS Sustain. Chem. Eng. 3 (2015) 1905–1914, https://doi.org/10.1021/acssuschemeng.5b00041.
[29] J. Wildschut, F.H. Mahfud, R.H. Venderbosch, H.J. Heeres, Hydrotreatment of fast pyrolysis oil using heterogeneous noble-metal catalysts, Ind. Eng. Chem. Res. 48 (2009) 10324–10334, https://doi.org/10.1021/ie9006003.
[30] W. Yin, A. Kloekhorst, R.H. Venderbosch, M.V. Bykova, S.A. Khromova, V. A. Yakovlev, H.J. Heeres, Catalytic hydrotreatment of fast pyrolysis liquids in batch and continuous set-ups using a bimetallic Ni–Cu catalyst with a high metal content, Catalysis Science & Technology 6 (2016) 5899–5915, https://doi.org/10.1039/C6CY00503A.
[31] P. de Wild, R.V. der Laan, A. Kloekhorst, E. Heeres, Lignin valorisation for chemicals and (transportation) fuels via (catalytic) pyrolysis and hydrodeoxygenation, Environ. Prog. Sustain. Energy 28 (2009) 461–469, https://doi.org/10.1002/ep.10391.
[32] D.J. McClelland, A.H. Motagamwala, Y. Li, M.R. Rover, A.M. Wittrig, C. Wu, J. S. Buchanan, R.C. Brown, J. Ralph, J.A. Dumesic, Functionality and molecular weight distribution of red oak lignin before and after pyrolysis and hydrogenation, Green Chem. 19 (2017) 1378–1389, https://doi.org/10.1039/C6GC03515A.
[33] J.I. Park, L. Liu, X. Philip Ye, M.K. Jeong, Y.-S. Jeong, Improved prediction of biomass composition for switchgrass using reproducing kernel methods with wavelet compressed FT-NIR spectra, Expert Syst. Appl. 39 (2012) 1555–1564, https://doi.org/10.1016/j.eswa.2011.05.012.